

Article

Experimental Evaluation of a Paraffin as Phase Change Material for Thermal Energy Storage in Laboratory Equipment and in a Shell-and-Tube Heat Exchanger

Jaume Gasia ¹, Laia Miró ¹, Alvaro de Gracia ², Camila Barreneche ^{1,3} and Luisa F. Cabeza ^{1,*}

¹ GREA Innovació Concurrent, Universitat de Lleida, Edifici CREA, Pere de Cabrera s/n, 25001 Lleida, Spain; jaume.gasia@diei.udl.cat (J.G.); lmiro@diei.udl.cat (L.M.); cbarreneche@diei.udl.cat (C.B.)

² Departament d'Enginyeria Mecànica, Universitat Rovira i Virgili, Av. Paisos Catalans 26, 43007 Tarragona, Spain; alvaro.degracia@urv.cat

³ Department of Materials Science and Metallurgical Engineering, Universitat de Barcelona, Martí i Franqués 1-11, Barcelona, Spain

* Correspondence: lcabeza@diei.udl.cat; Tel.: +34-973003576

Academic Editor: Mohammed Mehdi Farid

Received: 2 March 2016; Accepted: 8 April 2016; Published: 18 April 2016

Abstract: The thermal behavior of a commercial paraffin with a melting temperature of 58 °C is analyzed as a phase change material (PCM) candidate for industrial waste heat recovery and domestic hot water applications. A full and complete characterization of this PCM is performed based on two different approaches: a laboratory characterization (mass range of milligrams) and an analysis in a pilot plant (mass range of kilograms). In the laboratory characterization, its thermal and cycling stability, its health hazard as well as its phase change thermal range, enthalpy and specific heat are analyzed using a differential scanning calorimeter, thermogravimetric analysis, thermocycling and infrared spectroscopy. Laboratory analyses showed its suitability up to 80 °C and for 1200 cycles. In the pilot plant analysis, its thermal behavior was analyzed in a shell-and-tube heat exchanger under different heat transfer fluid mass flow rates in terms of temperature, power and energy rates. Results from the pilot plant analysis allowed understanding the different methods of heat transfer in real charging and discharging processes as well as the influence of the geometry of the tank on the energy transferred and required time for charging and discharging processes.

Keywords: thermal energy storage; latent heat; phase change material; paraffin; heat exchanger; shell-and-tube; laboratory; pilot plant

1. Introduction

According to the International Energy Agency [1], current trends in energy supply and use are economically, environmentally and socially unsustainable since energy-related emissions of carbon dioxide will be doubled by 2050 and fossil energy demand will increase over the security of supplies. Hence, researchers are forced to go deeper into finding materials and systems to make sure the presence of energy storage in the domestic sector, transport and industry to support energy security and climate change goals. Among the different energy storage technologies, thermal energy storage (TES) arises as a key technology to reduce the mismatch between energy demand and supply on a daily, weekly and even seasonal basis, increasing the potential of implementation of renewable energies and reducing the energy peak demand.

There are three technologies of TES: sensible, latent and thermochemical heat storage. The storage of energy within the sensible heat storage technology is linked to the rise of temperature of the TES

material, which can be either in liquid or solid state. In latent heat storage technologies, the thermal energy is stored when the TES material, also called phase change material (PCM), undergoes phase change processes. Finally, in thermochemical heat storage technologies, the energy is stored after a reversible chemical reaction between two substances.

Latent heat TES has been deeply studied during the past decades and it has been found to be nowadays more attractive than sensible heat storage despite the fact that, in terms of cost, sensible TES materials are cheaper than PCM because of their high storage densities and narrower operating temperatures [2], and more attractive than thermochemical heat storage because of their maturity. One of the most studied PCMs is paraffin [3], which is an organic PCM consisting of a mixture of straight chain *n*-alkanes $\text{CH}_3-(\text{CH}_2)_n-\text{CH}_3$. However, due to the high cost of manufacturing, only technical grade paraffins (mixtures of many hydrocarbons) are used for latent heat TES purposes [4]. Several studies have already reported and demonstrated the desirable properties of paraffins, which make this organic PCM suitable for TES [5]. From the thermal point of view, paraffins are known to have high thermal energy storage capacity, relatively constant melting temperatures close to the assumed phase change temperature, negligible subcooling and low vapor pressure in the melting process. Furthermore, paraffin is chemically inert and stable; it does not show phase segregation, it is non-corrosive to the container material, and it is commercially available. There are also some undesirable properties that limit the potential capabilities of this material. Such major drawbacks are: large volume changes during phase transition, compatibility problems with plastic containers, possibility of flammability, and low thermal conductivity. With some modifications in the wax and in the storage unit, all the undesirable effects mentioned before can be partially addressed and even eliminated [6].

Several experimental studies concerning the melting and solidification processes of different technical grade paraffin have been conducted, reporting their desirable properties. Trp [7] analyzed the behavior of paraffin RT-30 in a 48 L shell-and-tube heat exchanger during both melting and solidification processes using water as heat transfer fluid (HTF) at a single constant mass flow rate, observing that phase change occurred non-isothermally but within the melting zone. In a similar shell-and-tube heat exchanger, but under different mass flow rates and inlet HTF (water) temperatures, Rathod and Banerjee [8] studied the thermal behavior of a paraffin wax with a melting temperature of 60 °C, observing that inlet temperature had a higher effect on the heat fraction during the PCM melting than the mass flow rate. Moreover, Akgün *et al.* [9] studied melting and solidification processes of different commercial paraffins (P42–44, P46–48, P56–58), which were experimentally tested at laboratory (5 mg) and at higher scale (2.2 kg) in a shell-and-tube heat exchanger with an inclination angle of 5 °C for various inlet temperatures and mass flow rates of the HTF (water), and obtained similar conclusions as in the previous study. Furthermore, Jesumathy *et al.* [10,11] evaluated the thermal behavior of 0.7 kg of commercial paraffin in a shell-and-tube heat exchanger, placed both horizontally and vertically, under the influence of different HTF (water) mass flow rates and inlet temperatures during the melting and solidification processes. Results showed no subcooling of the paraffin and demonstrated that the modification of the HTF operating conditions has a higher influence during melting than during solidification. Medrano *et al.* [12] evaluated the temperature profiles and the power exchanged of commercial paraffin RT-35 in four different heat exchangers (0.35–1.1 kg of PCM) during melting and solidification processes working at two different volumetric flow rates and two different HTF (water) inlet temperatures. They observed that the increase of both the thermal gradient between HTF and the PCM, and the mass flow rate resulted in a decrease of the phase change time; therefore, an increase of the average heat transfer rate during charging and discharging processes. He and Setterwall [13] investigated the behavior of paraffin RT-5 for cold storage at laboratory scale (5 mg) and at a higher scale (100 mL) and the associated cost for its implementation at higher scale. Results showed that paraffin had congruent melting, no subcooling and good stability.

The aim of the present study is to perform a complete laboratory analysis of paraffin RT58 at both laboratory and pilot scale (around 15 mg and 108 kg, respectively). The laboratory characterization

includes the thermal and cycling stability, health hazard, differential scanning calorimetry (DSC), thermogravimetric analysis (TGA), and infrared (FT-IR) spectroscopy. In the pilot plant characterization scale, the thermal behavior of 108 kg of paraffin was analyzed in a shell-and-tube heat exchanger, with different HTF flow rates, in terms of temperature profiles, power exchanged and energy stored.

2. Materials Description

The selected PCM in the present study is the commercial paraffin RT58, commercialized by Rubitherm GmbH (Berlin, Germany). Table 1 shows the main thermo-physical properties of the material according to the manufacturer.

Table 1. Thermo-physical properties of RT58 according to the manufacturer.

Properties	Units	Values
Melting area	(°C)	53–59
Congealing area	(°C)	59–53
Heat storage capacity \pm 7.5% (combination of latent and sensible heat in a temperature range of 50 °C to 65 °C)	(kJ·kg ⁻¹)	160
	(Wh·kg ⁻¹)	48
Specific heat capacity	(kJ·(kg·K) ⁻¹)	2
Density solid (at 15 °C)	(kg·L ⁻¹)	0.88
Density liquid (at 80 °C)	(kg·L ⁻¹)	0.77
Heat conductivity (solid and liquid)	(W·(m·K) ⁻¹)	0.2
Volume expansion	(%)	12.5
Flash point (PCM)	(°C)	>200
Max. operation temperature	(°C)	80

Regarding the possible applications of RT58 and taking into account its melting thermal range, the most suitable applications are domestic hot water (DHW) [14] and low temperature industrial waste heat (IWH) recovery [15].

3. Laboratory Analyses

The laboratory methodology proposed by Miró *et al.* [16] to select a suitable PCM for a TES application is used. In previous studies, the selection of a PCM was based only on the phase change thermal range, the enthalpy and the specific heat. In this new methodology, a combination of thermal stability, health hazard and cycling stability is presented to complement previous analyses.

Differential scanning calorimeter (DSC) analyses were carried out to measure the phase change thermal range and the enthalpy of fusion along the range of temperatures in which the experimentation at pilot plant was performed. The equipment used to carry out the analysis was a DSC-822e commercialized by Mettler Toledo (Greifensee, Switzerland). A dynamic method analysis based on earlier studies [17] was performed. A sample of 12.8 mg sealed in a 40 μ L aluminium crucible was heated under an inert atmosphere of N₂ up from 20 °C to 75 °C at a heating rate of 0.5 °C/min and cooled back at the same range of temperatures and heating rate. The results obtained are compared and discussed against the ones provided by the manufacturer.

The thermal stability of the paraffin is analyzed using a thermogravimetric analysis (TGA). It measures weight changes in a material as function of temperature (or time) under a controlled atmosphere. The TGA was performed with a Simultaneous SDTQ600 from TA Instruments (New Castle, PA, USA) under nitrogen flow. The heating rate applied was 10 °C/min between 25 °C and 600 °C to a 30 mg sample size.

The cycling stability was analyzed to detect possible changes in the thermo-physical properties of the material along a certain amount of freezing/melting cycles. In the present study, the studied thermo-physical properties studied were the latent heat and the melting temperature. First, a cycling test (1200 cycles) was performed using a thermal cycler from Termociclador GENE Q Hangzhou BioerTechnology (Hangzhou, China). Three samples have been gathered each time after 500, 1000, and 1200 samples from an Eppendorf. The temperature program for one cycle was 1.5 min at 45 °C and 1.5 min at 70 °C to ensure full solidification and full melting during the cycle. The applied heating rate is the fastest: around 20 °C/min. Second, an evaluation of the cycled samples was performed using the same apparatus and methodology used for the DSC analysis.

Finally, the infrared (FT-IR) spectroscopy was carried out to study the chemical stability of the material after a certain amount of cycles. Its working principle is based on the measurement of the molecules bonds vibration under infrared light. FT-IR spectroscopy was performed using a Spectrum Two from Perkin Elmer (Waltham, MA, USA) and supported by a Dynascan interferometer (Perkin Elmer, Waltham, MA, USA) and OpticsGuard (Perkin Elmer, Waltham, MA, USA). This equipment performs IR spectra between 8300 and 350 cm^{-1} , and liquids and solid samples can be measured.

4. Pilot Plant Analyses

4.1. Experimental Setup

The facility used to experimentally test the PCM at a real scale was designed and built at the University of Lleida, and it is integrated by three parts: (1) the heating system, which consists of a 24 kW_e electrical boiler that heats up the HTF acting as the heating energy source during a charging process in a real installation; (2) the cooling system, which is based on a 20 kW_{th} air-HTF heat exchanger that simulates the energy consumption by the user during a discharging process in a real facility; and (3) the storage system, which consists of a stainless steel storage tank based on the shell-and-tube heat exchanger concept. The tank stores the thermal energy during the charging process and releases it during the discharging process. Figure 1 shows an overview of the pilot plant facility. All three systems are linked through a piping system that distributes the HTF: Syltherm 800 (Dow Heat Transfer Fluids, Midland, TX, USA). Moreover, rock wool and Foamglass (Pittsburgh Corning, Pittsburgh, PA, USA) are used as insulation to minimize the heat losses to the surroundings.



Figure 1. Overview of the pilot plant facility available at the University of Lleida and used in the experimentation.

To carry out an accurate analysis of the PCM thermal behavior and to get a precise map of temperatures during the charging and discharging processes, thirty-one temperature sensors PT-100

with an accuracy of ± 0.1 °C were installed inside the storage tank at different positions (Figure 2a). Nineteen of these probes were located in the main part (from $T_{PCM,1}$ to $T_{PCM,15}$), six probes were located in the corner part close to the U bend (from $T_{c,1}$ to $T_{c,6}$) and six probes were located at the central part (from $T_{in,1}$ to $T_{in,6}$). Each temperature sensor was associated to a control volume, which is defined as the theoretical volume of PCM in which the value of the temperature sensor could be stated as representative. Finally, two temperature sensors PT-100 were installed at the inlet and outlet of the HTF tubes bundle to measure the inlet and outlet HTF temperature. All the temperature sensors and HTF flow meters are connected to a data acquisition system, which controls, measures and records the information at a time interval of 30 s. Concerning to the distribution of the PCM inside the storage tank (Figure 2b), the biggest amount of material (78%) is located within the tubes bundle along the main part of the storage tank while the remaining 22% is located in the corners and in the central part of the tank.

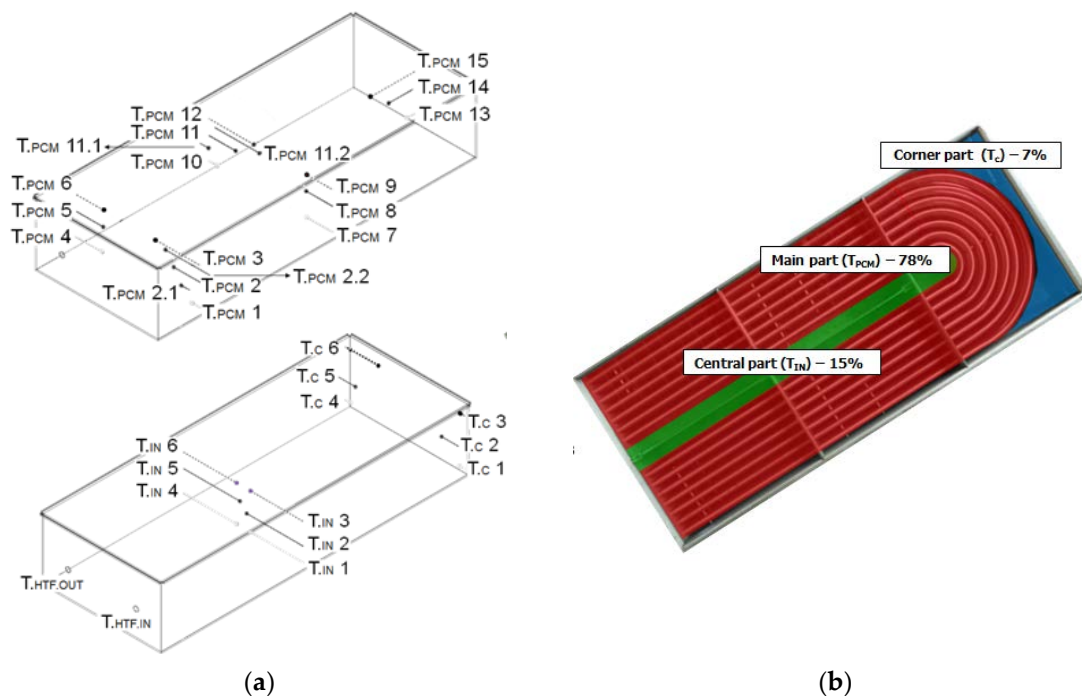


Figure 2. Storage system: (a) temperature sensors location at three different levels, highlighted in grey (lower), black (middle) and dotted (upper); (b) distribution of the phase change material (PCM) inside the storage tank colored in blue (corner part), red (main part) and green (central part).

4.2. Methodology

Different experiments comprising charging and discharging processes at a thermal range of 48 °C and 68 °C and at different constant HTF mass flow rates were performed. A narrow temperature range around the PCM melting temperature is selected to study the PCM behavior, mostly in the latent phase. The three different tested mass flow rates were 500 kg/h, considered as low flow, 1500 kg/h, considered as mid flow and 2500 kg/h, considered as high flow. Despite having a maximum mass flow rate of 2500 kg/h, only a laminar regime could be achieved because of the high viscosity of the HTF and the limitations of the pilot plant facility.

Before starting the charging process, a warming process was required to make the PCM be uniform and homogeneous at the initial temperature of charging. Once the PCM reached the initial temperature conditions for charging (48 °C), the HTF was heated up outside the tank up to the inlet HTF temperature (68 °C) and afterwards the charging process started. The charging process was considered to be finished once the difference between the inlet and outlet HTF temperature was less than 2 °C and the weighted average temperature of the middle temperature sensors reached 68 °C.

Then, a reverse process took place to carry out the discharging process (PCM initial temperature of 68 °C and HTF inlet temperature of 48 °C).

5. Results and Discussion

5.1. Laboratory Analyses

The first parameter analyzed by the authors was the health hazard from the RT58 material safety data sheet. According to standards 1272/2008 and 1999/45/EG, it represents no hazard.

Results from the DSC analysis (Figure 3) showed that the phase change temperature range is 50–61 °C with a peak temperature at 58.3 °C. Since RT58 is technical grade paraffin, the fact of observing a temperature range instead of a sharp melting point in the melting is coherent. The phase change enthalpy for the melting temperature range is found, from the DSC analysis, by numerical integration within the melting temperature range and results 120.1 kJ/kg far from the value presented by the manufacturer (Table 1). The reason might lie in the use of different techniques and methodology to determine it [17].

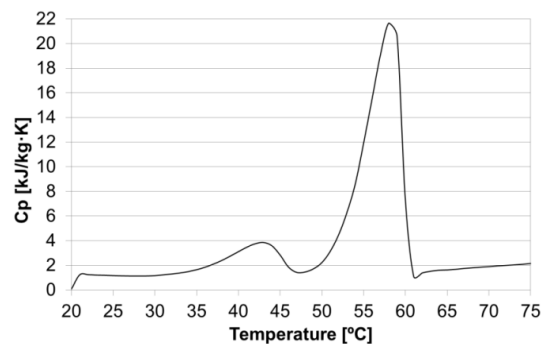


Figure 3. Differential scanning calorimeter (DSC) analysis of RT58.

Figure 4a shows the TGA of RT58. It can be seen that the sample degrades in one step. The paraffin degradation starts at 200 °C and it is finished at 350 °C, which allows for the conclusion that usage of RT58 should be avoided above 200 °C. Since the temperature range of the potential applications and the present experimentation is far away from the beginning of the degradation, no problem regarding this matter was expected during the present experimentation. If this result is compared against the thermo-physical properties presented by the manufacturer (Table 1), the obtained results match with the manufacturer data sheet (Flash point > 200 °C). However, it has to be noticed that the maximum operational temperature of RT58 is 80 °C due to its vapor pressure. Hence, an appropriate control system should be used to avoid the operation of the PCM above these thermal conditions.

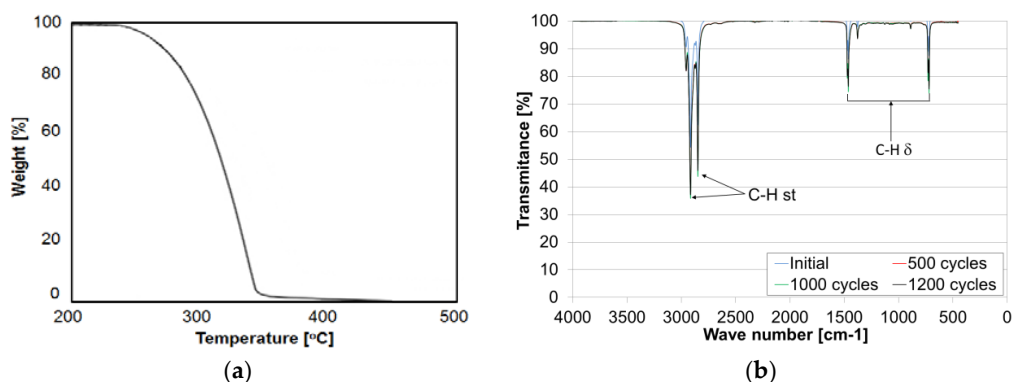


Figure 4. RT58 laboratory analyses results: (a) Thermogravimetric analysis (TGA); (b) Infrared (FT-IR) spectroscopy before and after 500, 1000 and 1200 cycles.

Figure 4b shows the FT-IR spectrograms of an RT58 sample before and after 500, 1000 and 1200 cycles and the FT-IR characteristic peaks of this kind of materials. Results show that RT58 presents non-chemical degradation since they show equal FT-IR characteristic peaks with similar profiles.

Furthermore, samples after 500, 1000 and 1200 cycles were taken to study the evolution of the phase change temperature and latent heat of the studied material. Results are presented in Table 2, and show that after 1200 cycles, the variation on the phase change temperature is about 1.7% and the variation on the latent heat is about 2.7%, meaning that paraffin RT58 presents no degradation after 1200 cycles. The lack of a clear and consistent pattern in the enthalpy values along the cycles may be due to the DSC error itself along with differences between the DSC samples and cycling conditions (mass, pan, sample preparation, or the presence of humidity in the DSC). This kind of behavior has been widely seen in various studies involving different materials [18].

Table 2. Thermo-physical properties of RT58 before and after 500, 1000 and 1200 cycles.

Property	Units	Initial 0 Cycles	500 Cycles	1000 Cycles	1200 Cycles
Phase change Temperature	(°C)	58.3	58.8	58.6	57.3
Latent heat	(J/g)	204.2	255.5	242.9	209.9

5.2. Pilot Plant Analyses

5.2.1. Temperature Evolution

Figure 5 shows the temperature evolution of the HTF at the inlet and outlet of the tank and the temperature profiles of the mid-height control volumes of the PCM (Figure 2a) during the charging and discharging processes at a HTF mass flow rate of 1500 kg/h.

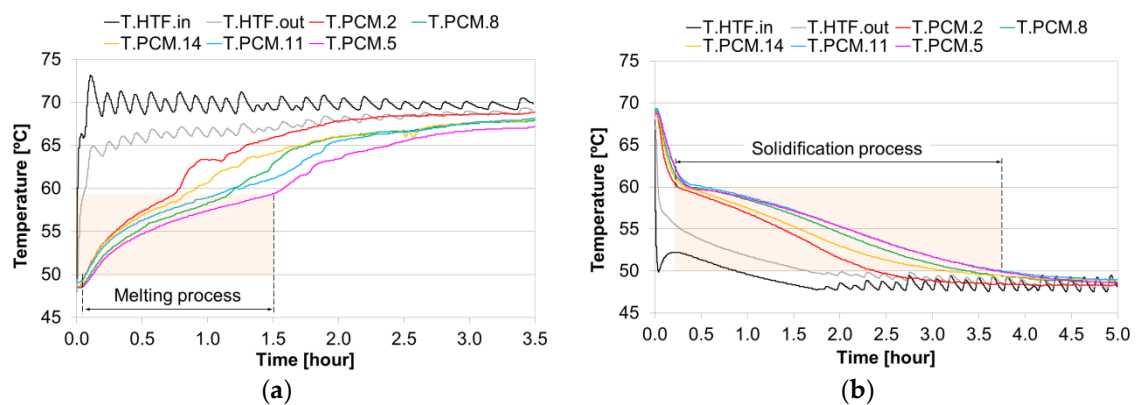


Figure 5. PCM and heat transfer fluid (HTF) temperature profile at an HTF mass flow rate of 1500 kg/h: (a) charging process and (b) discharging process. Shaded area indicates the melting and the solidification temperature range.

During the charging process (Figure 5a), the PCM located at the beginning of the tubes bundle and controlled by the temperature sensor $T_{PCM,2}$ achieved higher temperatures with less time, since the energy supplied by the HTF was received during the first stage, and, therefore, started and finished the melting and charging processes before the rest of the PCM located along the tank. The PCM located at the end of the tube bundle and controlled by the temperature sensor $T_{PCM,5}$ had the opposite behavior for analogous reason. From the first seven minutes (0.12 h), the PCM started to melt at a temperature of 50 °C; after 100 min (1.67 h) of experimentation, when the PCM reached 59 °C, the melting process was finished, and after 209 min (3.5 h), the charging process was completed. During the discharging process (Figure 5b), it can be seen that the solidification started 15 min (0.25 h) after starting the process, when the PCM reached 60 °C, and the PCM was fully solidified after 190 min (3.16 h), when the PCM

reached 50 °C. The discharging process was terminated after 296 min (4.93 h). Comparing the two processes, it was observed that the discharge was 42% slower than the charge. The main reasons for these differences in time lie in the presence of natural convection during the melting process, which enhanced the charging process and the creation of a solid layer around the tubes bundle when the PCM started to solidify, which hindered the discharging process. Furthermore, the upper value of the melting temperature range of the sample analyzed at pilot plant scale lie is 1–2 °C lower than the value obtained from the DSC analysis, while the lower value was the same in both cases.

Figure 6 provides the comparison between the three evaluated mass flow rates (500, 1500 and 2500 kg/h), showing the temperature profiles of two representative PCM temperature sensors ($T_{PCM,2}$ and $T_{PCM,11}$) during a charging and a discharging process. Notice that in both processes, the higher the mass flow rates were, the faster the PCM reached the desired temperatures, demonstrating the influence of the mass flow rate on the PCM heating rate. The reason lies in the fact that the heat transfer from the HTF to the first layer of PCM is dominated by the convection mechanism. Although the heat transfer coefficient remains constant in the different evaluated flow rates (fully developed internal laminar flow), the temperature difference between the HTF and the PCM is the parameter that determines the influence of the flow rate on the heat transfer rate.

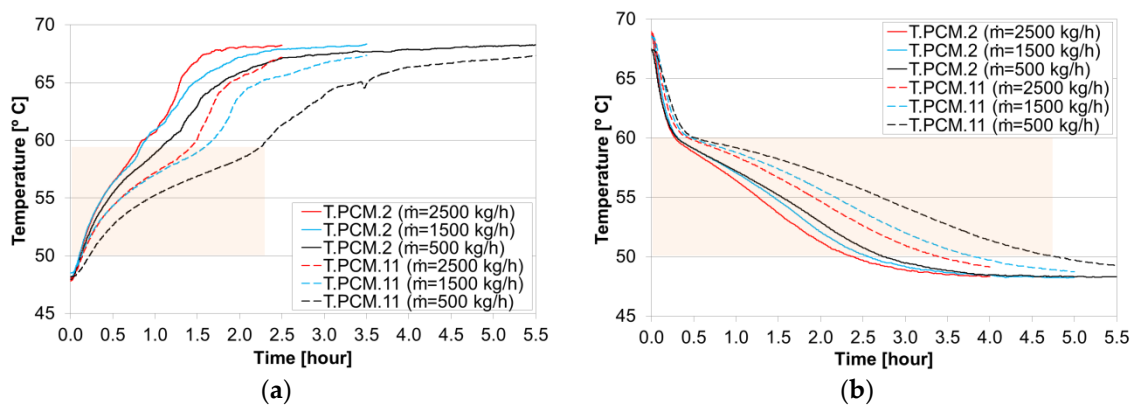


Figure 6. Comparison of the temperature profiles of two representative PCM temperature sensors with three different mass flow rates. (a) charging process and (b) discharging process. Shaded area indicates the melting and the solidification temperature range.

5.2.2. Power Profile

Figure 7 shows the power released/absorbed by the HTF and the PCM and HTF average temperature profiles during the charging and discharging processes at an HTF mass flow rate of 1500 kg/h. At the beginning of both processes, higher values of power were achieved because the heat was mainly transferred to the metallic tubes bundle, which has a high thermal conductivity, and at the same time the heat transfer between the HTF and the PCM located around the HTF pipes was at a maximum because the PCM thermal resistance was low and the thermal gradient between the HTF and the PCM was at a maximum. Immediately after, when the PCM started the phase change, the power drastically decreased due to the increase of the PCM thermal resistance. The reason lies in the fact that the PCM melting front moved away from the HTF as the phase change continued and therefore increased the distance between the HTF and the PCM melting. Focused on the charging process (Figure 7a), a liquid ring was created around the HTF pipes, and, therefore, the natural convection became the predominant heat transfer mechanism. As the process continued, the liquid fraction of PCM increased and, consequently, the thermal conductivity associated, until all the heat transfer was aimed to increase the temperature of the PCM located at the corners and the central part of the tank. During the discharging process (Figure 7b), a more sharp decrease could be observed. The reason lies in the fact that a solid PCM ring was created around the HTF pipes, which limited the heat transfer since the thermal conductivity became the dominant heat transfer mechanism.

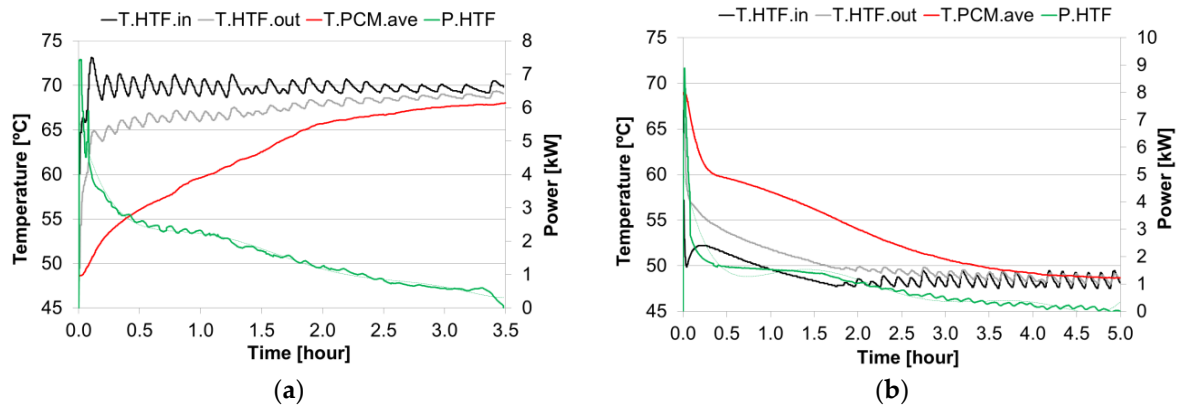


Figure 7. HTF power profiles and average PCM and HTF temperature profiles at an HTF mass flow rate of 1500 kg/h: (a) charging process and (b) discharging process.

Figure 8 shows the comparison between the three evaluated mass flow rates (500, 1500 and 2500 kg/h) of the power released/recovered by/from the HTF during a charging and a discharging process. It can be observed that at the beginning of both processes, the higher the mass flow rate, the higher the power as previously detailed. However, as the processes continued, the thermal gradient between HTF and PCM decreased and the influence of the mass flow did not become as relevant.

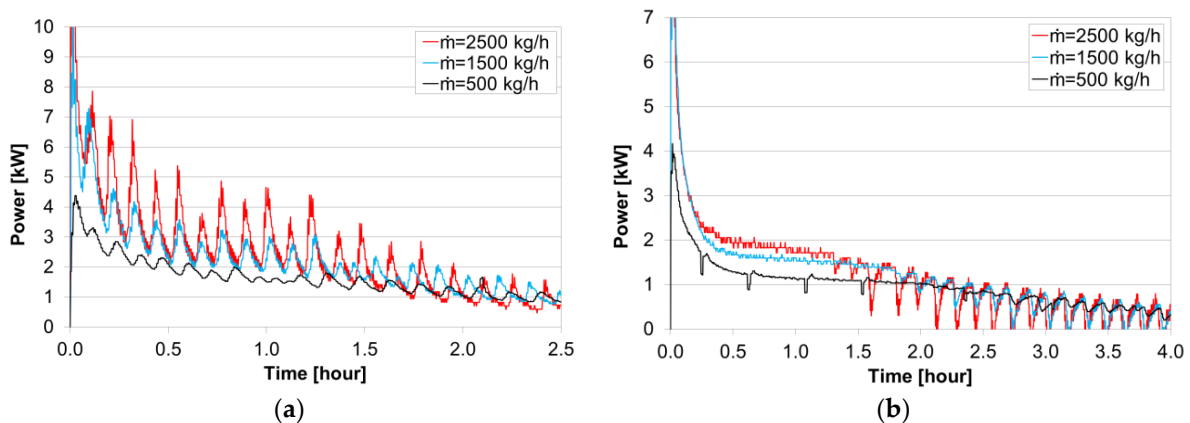


Figure 8. Comparison of the HTF power profiles with three different mass flow rates. (a) charging process and (b) discharging process.

5.2.3. Energy Profile

Because of the non-linear evolution of the energy accumulated/released by the PCM during full charging and discharging processes, and in order to extrapolate the results for other processes which are more likely to happen in a real installation, such as partial charging and discharging processes, an important parameter to be evaluated is the energy rate. This parameter is a ratio between the energy accumulated along the specific process and the final energy that the system has accumulated at the moment when the process is considered being finished. Hence, this rate always achieves 100% at the end of the process. This information is useful to understand how the geometry of the tank influences the charging and discharging processes.

Figure 9 shows the energy rate, bearing in mind the distribution of the PCM inside the tank (Figure 2b), during the charging and discharging processes for an HTF mass flow rate of 1500 kg/h. It can be observed that the PCM located at the main part accumulates/releases the energy faster than the other parts because it exchanges the energy with the HTF easier as they are in direct contact with the tubes bundle, while the PCM located at the corners takes much more time to start storing/releasing

the energy. This situation shows a non-optimized design of the heat exchanger and, in order to enhance the heat transfer, the corners should be avoided. In both processes, the PCM took around 50% of the process time to accumulate/release 90% of the energy, which is a good reference for partial load processes such as the ones driven by intermittent renewable energies because it can lead on one hand to a redesign of the charging and discharging process, and on the other hand to a redesign of the storage tank.

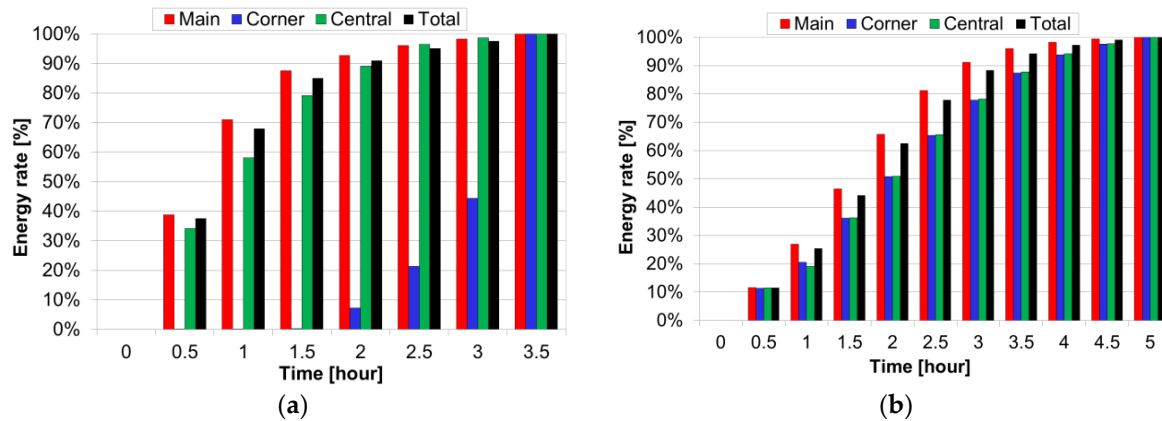


Figure 9. Evolution of the PCM energy rate taking into account the central, main and corner parts of the tank as well as for the whole tank at an HTF mass flow rate of 1500 kg/h: (a) charging process and (b) discharging process.

In the present study, if compared to the processes at a mass flow rate of 500 kg/h, the process at a mass flow rate of 2500 kg/h was 62% faster during the discharge and 124% faster during the charge, while the process at a mass flow rate of 1500 kg/h was 29% faster during the discharge and 60% faster during the charge times faster. The differences observed between the charging and discharging are mainly due to the dominant heat transfer mechanisms—while, during the charging process, it is mainly the convection, and during the discharging process it is the conduction.

6. Conclusions

A full characterization of a commercial paraffin with a melting temperature of 58 °C is performed from two different approaches: a laboratory characterization (mass range of milligrams) and a pilot plant characterization (mass range of kilograms). The analyzed PCM is selected as a candidate for industrial waste heat recovery and domestic hot water applications.

In the laboratory characterization, the thermal and cycling stability of the paraffin, its health hazards as well as its phase change thermal range, enthalpy and specific heat are analyzed using a differential scanning calorimeter, thermogravimetric analysis, thermocycling and infrared spectroscopy. Results showed no health hazards, with a phase change temperature range of 50–61 °C and enthalpy of 120.11 kJ·kg⁻¹. Thermal and cycling stability tests showed that this paraffin is suitable for its use up to 80 °C and presents no degradation after 1200 cycles.

At the pilot plant facility, the characterization of 108 kg of PCM was analyzed in a shell-and-tube heat exchanger under different HTF mass flow rates, in terms of temperature profiles, power released/absorbed and energy rates during charging and discharging processes. Comparing the temperature profiles of the two processes, it was observed that the discharge showed a slower response than the charge because of the presence of natural convection during the melting process and the creation of a solid layer around the tube bundle when the solidification process is started. The duration of the charging and discharging process was also affected by the different HTF mass flow rates. Regarding the power released/absorbed, at the beginning of both processes, the higher the mass flow rate, the higher the power. However, as the processes continued, this temperature gradient

decreased and the influence of the mass flow did not become as relevant. Finally, it was showed that the energy rate is an important parameter to be tested because of the non-linearity evolution of the energy accumulated/released by the PCM, which also indicates how optimal the design of a TES tank is. This last parameter will be studied deeply by the authors in further work.

Acknowledgments: The work is partially funded by the Spanish government (ULLE10-4E-1305, ENE2015-64117-C5-1-R and ENE2015-64117-C5-3-R). This project has received funding from the European Commission Seventh Framework Programme (FP/2007–2013) under Grant agreement N°PIRSES-GA-2013-610692 (INNOSTORAGE) and No ENER/FP7/295983 (MERITS), and from the European Union’s Horizon 2020 Research and Innovation Programme under Grant agreement No 657466 (INPATH-TES). The authors would like to thank the Catalan Government for the quality accreditation given to their research groups GREA (2014 SGR 123) and DIOPMA (2014 SGR 1543). Jaume Gasia would like to thank the Departament d’Universitats, Recerca i Societat de la Informació de la Generalitat de Catalunya for his research fellowship (2016FI_B 00047). Laia Miró would like to thank the Spanish Government for her research fellowship (BES-2012-051861). Alvaro de Gracia and Camila Barreneche would like to thank the Ministerio de Economía y Competitividad de España for Grant Juan de la Cierva, FJCI-2014-19940 and FJCI-2014-22886, respectively.

Author Contributions: Jaume Gasia, Laia Miró and Luisa F. Cabeza conceived and designed the study; Jaume Gasia performed the experiments at pilot plant scale and Camila Barreneche performed the experiments at the laboratory scale; all the coauthors collaborated on the interpretation of the results and on the preparation of the manuscript.

Conflicts of Interest: The authors declare no conflict of interest.

References

1. International Energy Agency. Technology Roadmap: Energy Storage. Available online: <https://www.iea.org/publications/freepublications/publication/technology-roadmap-energy-storage.html> (accessed on 13 May 2015).
2. Mehling, H.; Cabeza, L.F. *Heat and Cold Storage with PCM: An up to Date Introduction into Basics and Applications*, 1st ed.; Springer Science & Business Media: Berlin, Germany, 2008; pp. 11–57.
3. Zalba, B.; Marín, J.M.; Cabeza, L.F.; Mehling, H. Review on thermal energy storage with phase change: Materials, heat transfer analysis and applications. *Appl. Therm. Eng.* **2003**, *23*, 251–283.
4. Sharma, A.; Tyagi, V.V.; Chen, C.R.; Buddhi, D. Review on thermal energy storage with phase change materials and applications. *Renew. Sustain. Energy Rev.* **2009**, *13*, 318–345. [[CrossRef](#)]
5. Farid, M.M.; Khudhair, A.M.; Razack, S.A.K.; Al-Hallaj, S. A review on phase change energy storage: Materials and applications. *Energy Convers. Manag.* **2004**, *45*, 1597–1615. [[CrossRef](#)]
6. Hasnain, S.M. Review on sustainable thermal energy storage technologies, Part I: Heat storage materials and techniques. *Energy Convers. Manag.* **1998**, *39*, 1127–1138. [[CrossRef](#)]
7. Trp, A. An experimental and numerical investigation of heat transfer during technical grade paraffin melting and solidification in a shell-and-tube latent thermal energy storage unit. *Sol. Energy* **2005**, *79*, 648–660. [[CrossRef](#)]
8. Rathod, M.K.; Banerjee, J. Experimental Investigations on Latent Heat Storage Unit using Paraffin Wax as Phase Change Material. *Exp. Heat Transf.* **2014**, *27*, 40–55. [[CrossRef](#)]
9. Akgün, M.; Aydın, O.; Kaygusuz, K. Thermal energy storage performance of paraffin in a novel tube-in-shell system. *Appl. Therm. Eng.* **2008**, *28*, 405–413. [[CrossRef](#)]
10. Jesumathy, S.P.; Udayakumar, M.; Suresh, S. Heat transfer characteristics in latent heat storage system using paraffin wax. *J. Mech. Sci. Technol.* **2012**, *26*, 959–965. [[CrossRef](#)]
11. Jesumathy, S.P.; Udayakumar, M.; Suresh, S.; Jegadheeswaran, S. An experimental study on heat transfer characteristics of paraffin wax in horizontal double pipe heat latent heat storage unit. *J. Taiwan Inst. Chem. Eng.* **2014**, *45*, 1298–1306. [[CrossRef](#)]
12. Medrano, M.; Yilmaz, M.O.; Nogués, M.; Martorell, I.; Roca, J.; Cabeza, L.F. Experimental evaluation of commercial heat exchangers for use as PCM thermal storage systems. *Appl. Energy* **2009**, *86*, 2047–2055. [[CrossRef](#)]
13. He, B.; Setterwall, F. Technical grade paraffin waxes as phase change materials for cool thermal storage and cool storage systems capital cost estimation. *Energy Convers. Manag.* **2002**, *43*, 1709–1723. [[CrossRef](#)]
14. Kousksou, T.; Bruel, P.; Cherreau, G.; Leousoff, V.; El Rhafiki, T. PCM storage for solar DHW: From an unfulfilled promise to a real benefit. *Sol. Energy* **2011**, *85*. [[CrossRef](#)]

15. Brückner, S.; Liu, S.; Miró, L.; Radspieler, M.; Cabeza, L.F.; Lävemann, E. Industrial waste heat recovery technologies: An economic analysis of heat transformation technologies. *Appl. Energy* **2015**, *151*, 157–167. [[CrossRef](#)]
16. Miró, L.; Barreneche, C.; Ferrer, G.; Solé, A.; Martorell, I.; Cabeza, L.F. Health hazard, cycling and thermal stability as key parameters when selecting a suitable Phase Change Material (PCM). *Thermochim. Acta* **2016**, *627–629*, 39–47. [[CrossRef](#)]
17. Barreneche, C.; Solé, A.; Miró, L.; Martorell, I.; Fernández, A.I.; Cabeza, L.F. Study on differential scanning calorimetry analysis with two operation modes and organic and inorganic phase change material (PCM). *Thermochim. Acta* **2013**, *553*, 23–26. [[CrossRef](#)]
18. Ferrer, G.; Solé, A.; Barreneche, C.; Martorell, I.; Cabeza, L.F. Review on the methodology used in thermal stability characterization of phase change materials. *Renew. Sustain. Energy Rev.* **2015**, *50*, 665–685. [[CrossRef](#)]



© 2016 by the authors; licensee MDPI, Basel, Switzerland. This article is an open access article distributed under the terms and conditions of the Creative Commons Attribution (CC-BY) license (<http://creativecommons.org/licenses/by/4.0/>).